Inorganic Chemistry
Article

Inorg. Chem. 2009, 48, 7537–7543 7537
DOI: 10.1021/ic9001253

High-Pressure Phase Transition to the Gd_2S_3 Structure in Sc_2O_3: A New Trend in Dense Structures in Sesquioxides

Hitoshi Yusa,*,† Taku Tsuchiya,‡ Nagayoshi Sata,§ and Yasuo Ohishi||

†*Advanced Nano Materials Laboratory (ANML), National Institute for Materials Science (NIMS), 1-1 Namiki, Tsukuba 305-0044, Japan,* ‡*Geodynamics Research Center (GRC), Ehime University, 2-5 Bunkyo-cho, Matsuyama 790-8577, Japan,* §*Institute for Frontier Research on Earth Evolution (IFREE), Japan Agency for Marine−Earth Science and Technology (JAMSTEC), 2-15 Natsushima-cho, Yokosuka 237-0061, Japan, and* ||*Japan Synchrotron Radiation Research Institute (JASRI), 1-1-1 Kouto, Sayo-cho 679-5198, Japan*

Received January 21, 2009

In situ X-ray diffraction experiments using a laser-heated diamond anvil cell revealed a novel dense phase with the Gd_2S_3 structure stabilizing in Sc_2O_3 at pressures over 19 GPa. Although no phase transformation was induced during room-temperature compression up to 31 GPa, the C rare earth sesquioxide structure transformed into the B rare earth sesquioxide structure at 10 GPa after laser annealing and subsequently into the Gd_2S_3 structure at 19 GPa. Neither the A rare earth sesquioxide structure nor the U_2S_3 structure was found in Sc_2O_3. Static density functional lattice energy calculations demonstrated that the C structure prefers Gd_2S_3 over U_2S_3 as the post phase. Sc_2O_3 is the second sesquioxide, after In_2O_3, to crystallize into a Gd_2S_3 structure at high pressures and high temperatures.

Introduction

Scandium sesquioxide is a key component in synthesizing stabilized zirconia, which has high electrical conductivities available for solid oxide fuel cell applications.[1] It is also promising material for lanthanoid-doped solid-state lasers (e.g., Yb^{3+}:Sc_2O_3) emitting in the 1 μm region.[2] However, the high-pressure phase evolution of Sc_2O_3 is still highly unclear. Lanthanoid sesquioxides (Ln_2O_3) have been shown to have the phase sequence, C, B, and A, of rare earth sesquioxide structures (denoted as C-, B-, and A-RES, hereafter) with increasing temperature or pressure.[3−6] The C- to B-RES phase transition in scandium sesquioxide was reported to occur at 13 GPa in high P,T experiments using a Bridgman-type apparatus.[7] However, no further high-pressure form of Sc_2O_3 has been found to date. In shock-compression experiments,[8] recovered samples shocked at 20 and 40 GPa exhibited no diffraction peaks, but did exhibit broad diffractions corresponding to the C-RES phase, suggesting the existence of an unquenchable high-pressure phase. Subsequent Hugoniot measurements showed a large density increase of 11.5%,[9] and the authors concluded that the unquenchable phase has the A-RES structure transformed from C-RES at 40.9 GPa. They suggested that this transition pressure was consistent with the tendency known in other lanthanoid sesquioxides. Namely, the transition pressure of A-RES linearly increases as the cationic radius decreases. However, no in situ high-pressure X-ray experiment has been performed to confirm the results of this early shock-compression study so far. Considering the small effective cationic radius and absence of 4f electrons in Sc, scandium sesquioxide more closely resembles group 13 sesquioxides, such as In_2O_3, Tl_2O_3, and Ga_2O_3. So, we cannot expect the transition sequence of Ln_2O_3 to be simply applicable to Sc_2O_3. In fact, the corundum phase, which has been never found in Ln_2O_3, stabilizes at 6.5 GPa in Sc_2O_3−In_2O_3 solid solutions.[10]

Unlike rare earth sesquioxides, a lot of high-pressure studies have been done on group 13 sesquioxides. They recently elucidated high-pressure transition sequences from corundum to the Rh_2O_3(II) phase in Al_2O_3,[11−13]

*To whom correspondence should be addressed. E-mail: yusa.hitoshi@nims.go.jp.

(1) Mizutani, Y.; Tamura, M.; Kawai, M. *Solid State Ionics* **1994**, *72*, 271.
(2) Tokurakawa, M.; Shirakawa, A.; Ueda, K.; Yagi, H.; Yanagitani, T.; Kaminskii, A. A. *Opt. Lett.* **2007**, *32*, 3382.
(3) Goldschmidt, V.; Ulrich, F.; Barth, T. *Skr. Nor. Vidensk. Akad., Kl. 1: Mat. Naturvindensk. Kl.* **1925**, 5.
(4) Hoekstra, H.; Gingerich, K. *Science* **1964**, *146*, 1163.
(5) Sawyer, J. O.; Hyde, B. G.; Eyring, L. R. *Inorg. Chem.* **1965**, *4*, 427.
(6) Hoekstra, H. *Inorg. Chem.* **1966**, *5*, 754.
(7) Reid, A. F.; Ringwood, A. E. *J. Geophys. Res.* **1969**, *74*, 3238.
(8) Atou, T.; Kusaba, K.; Fukuoka, K.; Kikuchi, M.; Syono, Y. *J. Solid State Chem.* **1990**, *89*, 378.
(9) Atou, T.; Kikuchi, M.; Fukuoka, K.; Syono, Y. *AIP Conf. Proc.* **1994**, *309*, 331.
(10) Prewitt, C. T.; Shannon, R.; Rogers, D. B.; Sleight, A. W. *Inorg. Chem.* **1969**, *8*, 1985.
(11) Lin, J.; Degtyareva, O.; Prewitt, C.; Dera, P.; Sata, N.; Gregoryanz, E.; Mao, H. K.; Hemley, R. *Nat. Mater.* **2004**, *3*, 389.
(12) Thomson, K.; Wentzcovitch, R.; Bukowinski, M. *Science* **1996**, *274*, 1880.
(13) Duan, W.; Wentzcovitch, R.; Thomson, K. *Phys. Rev. B* **1998**, *57*, 10363.

Published on Web 04/14/2009

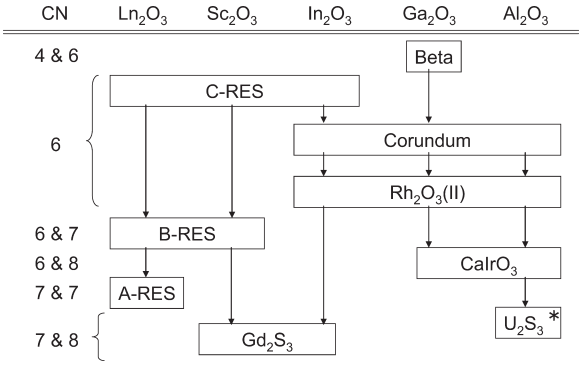

Figure 1. Phase transformation sequence of scandium sesquioxide, group 13 sesquioxides, and lanthanoid sesquioxides with their oxygen-coordination numbers (CNs) of cations. The asterisk denotes theoretical only.

Ga_2O_3,[14] and In_2O_3[14] (Figure 1). Furthermore, post-Rh_2O_3(II) phase transitions to the $CaIrO_3$ structure[15−17] have been discovered in Al_2O_3 and Ga_2O_3 in connection with the post perovskite phase in ternary compounds.[18,19] Most recently, the systematics of the post-$CaIrO_3$ phase transition have become one of the major research targets of high-pressure crystallography.[20,21] Ab initio density functional theory (DFT) computations predict a transition to the U_2S_3-type structure[22,23] in Al_2O_3 under extremely high pressure exceeding 370 GPa.[20] We experimentally discovered a transition to the Gd_2S_3 structure in In_2O_3 at about 40 GPa, with theoretical confirmations for this structure being much denser than the $CaIrO_3$ structure.[21] These findings of the sesquisulfide structures adoptable to new high-pressure sesquioxide phases are striking. Cations in both structures occupy seven and eight oxygen-coordinated sites, whereas cations in C, B, and A-RES structures occupy six, six and seven, and seven oxygen-coordinated sites, respectively. In terms of the high coordination number, both sesquisulfide structures of Gd_2S_3 and U_2S_3 are thought to be reasonable candidates for the post-C- and B-RES phases, not only for the post-$CaIrO_3$ and A-RES phases.

In the present study, we conducted in situ X-ray experiments at pressures up to 65 GPa to explore the phase evolution of Sc_2O_3. We also performed DFT computations with the local density approximation (LDA) and generalized-gradient approximation (GGA) to confirm the stability of known sesquioxide phases including A-RES, B-RES, corundum, Rh_2O_3(II), and $CaIrO_3$ phases in addition to the Gd_2S_3 and U_2S_3 phases mentioned above.

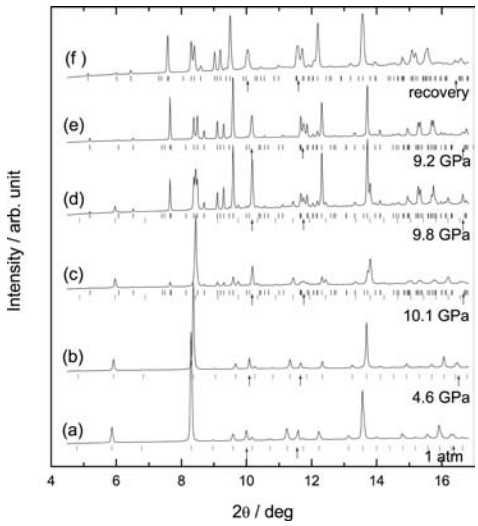

Figure 2. X-ray diffraction profiles from samples (a) at ambient pressure, (b) at 4.6 GPa after heating at 1500 ± 200 K, (c) at 10.1 GPa after heating at 1450 ± 200 K, (d) at 9.8 GPa after heating at 1550 ± 200 K, (e) at 9.2 GPa after heating at 1700 ± 200 K, and (f) after recovery at ambient pressure. Monochromatic X-ray radiation of 30 keV was used. Vertical bars represent the calculated positions of the diffraction peaks of the C-RES (lower bars) and B-RES (upper bars) structures. Arrows indicate the positions of diffraction from gold powder.

Experimental and Computational Procedures

High-Pressure Experiments. Powder of a scandium oxide sample (99.999% pure: Aldrich P/N 29, 402-0) was dried at 600 °C for 3 h in a furnace and used for the high-pressure experiments. The X-ray diffraction pattern recorded at ambient pressure in Figure 2a is of the starting sample having a crystalline C-RES phase without any other phase present. The symmetric diamond anvil cell (DAC) with a culet diameter of 0.3−0.4 mm generated pressures up to 65 GPa. A mixture of the scandium oxide sample and a small amount of gold powder (less than 0.01 wt %) was put into a hole drilled in a preindented rhenium gasket of 0.06 mm thickness. No pressure medium was used in laser heating experiments, in order to avoid unexpected reactions with the sample. The room-temperature compression experiments used a methanol/ethanol/water (16:3:1) mixture or an argon pressure medium.

The in situ X-ray diffraction experiments using the laser heating setup were conducted at BL10XU of SPring-8 (JASRI). A monochromatic X-ray beam (30 keV) was focused and collimated to a 20 μm spot size on the sample. Diffracted X-rays were detected by using an imaging plate (IP) and a charge-coupled device. A conical-hole (60°) tungsten carbide seat was placed under the 2-mm-high diamond anvil in order to pass the Debye rings on to the detectors within 20° in 2θ. The Fit2D program then converted the Debye rings into one-dimensional data (intensity vs 2θ).[24] The double-sided laser heating technique was used to get a high temperature. The heating experiments used a multimode continuous wave Nd:YAG laser with a 40 μm focused beam (Lee laser Inc.). Laser power of approximately 15−30 W heated the sample in the DAC to a maximum of 2500 K. The temperature was monitored during heating by measuring the spectrum of the radiation emitted from the sample.[25] The temperature uncertainty within a 20-μm area was about ±10%.[26] Pressure was determined from the

(14) Yusa, H.; Tsushiya, T.; Sata, N.; Ohishi, Y. *Phys. Rev. B* **2008**, *77*, 064107.
(15) Tsuchiya, J.; Tsuchiya, T.; Wenzcovitch, R. *Phys. Rev. B* **2005**, *72*, 020103(R).
(16) Ono, S.; Oganov, A.; Koyama, T.; Shimizu, H. *Earth Planet. Sci. Lett.* **2006**, *246*, 326.
(17) Tsuchiya, T.; Yusa, H.; Tsuchiya, J. *Phys. Rev. B* **2007**, *76*, 174108.
(18) Murakami, M.; Hirose, K.; Kuwayama, K.; Sata, N.; Ohishi, Y. *Science* **2004**, *304*, 855.
(19) Tsuchiya, T.; Tsuchiya, J.; Umemoto, K.; Wentzcovitch, R. M. *Earth Planet. Sci. Lett.* **2004**, *224*, 241.
(20) Umemoto, K.; Wentzcovitch, R. M. *Proc. Natl. Acad. Sci. U. S. A.* **2008**, *105*, 6526.
(21) Yusa, H.; Tsuchiya, T.; Tsuchiya, J.; Sata, N.; Ohishi, Y. *Phys. Rev. B* **2008**, *78*, 092107.
(22) Hoffman, W. *Z. Krystallogr.* **1933**, *86*, 225. U_2S_3 might have the same structure as Sb_2S_3, first reported in this article.
(23) Zachariasen, W. *Acta Crystallogr.* **1949**, *2*, 291.
(24) Hammersley, A. P. *European Synchrotron Radiation Facility Internal Report, ESRF97HA02T*; European Synchrotron Radiation Facility: Grenoble, France, 1997.
(25) Watanuki, T.; Shimomura, O.; Yagi, T.; Kondo, T.; Isshiki, M. *Rev. Sci. Instrum.* **2001**, *72*, 1289.
(26) Kurashina, T.; Hirose, K.; Ono, S.; Sata, N.; Ohishi, Y. *Phys. Earth Planet. Int.* **2004**, *145*, 67.

lattice parameters of gold.[27] The X-ray data were mainly collected at room temperature after heating. The experimental setup enabled the diffraction data to be taken during heating. However, the diffraction patterns recorded at high temperatures did not show any other new peaks but, rather, only a broadening of diffraction lines caused by a vertical thermal gradient in the sample.[28]

The room-temperature compression experiments were done at BL04B2 of SPring-8. A high-energy monochromatic X-ray beam (38 keV) was irradiated on a sample in a DAC with a 50 μm beam spot. The IP was used to detect the diffracted X-rays. The Debye rings recorded on the IP were processed in the same manner as at BL10XU.

Ab Initio Computations. Computations were performed within the framework of DFT[29] with LDA[30,31] and GGA[32] implemented in the PWSCF code.[33] Ultrasoft pseudopotentials for the scandium $3s^2 3p^6 3d^1 4s^2$ configuration and oxygen $2s^2 2p^6$ configuration were generated nonempirically using the method of Vanderbilt[34] with core radii of 1.8 au for Sc and 1.2 for O. A plane wave basis set with a cutoff of 50 Ry was used to compute the electronic structures of Sc_2O_3 polymorphs, and the irreducible parts of the Brillouin zone were sampled on $4 \times 4 \times 4$ (10 points), $2 \times 2 \times 2$ (2 points), $4 \times 4 \times 2$ (4 points), $4 \times 4 \times 4$ (10 points), $2 \times 2 \times 2$ (2 points), $4 \times 4 \times 2$ (4 points), and $2 \times 4 \times 2$ (2 points) Monkhorst−Pack meshes[35] for A-RES, B-RES, corundum, Rh_2O_3(II), $CaIrO_3$, Gd_2S_3, and U_2S_3 structures, respectively. All structural degrees of freedom were optimized using the variable cell-shape constant-pressure damped molecular dynamics technique until residual forces became less than 1.0×10^{-5} Ry/au. The effects of using a larger cutoff and a greater number of k points on the calculated properties were found to be insignificant.

Results and Discussion

Experimental Results. The starting C-RES sample was repeatedly laser-heated with a stepwise pressure increase. The first sign of a phase transition appeared at 10.1 GPa after heating at 1450 ± 200 K for about 30 s (Figure 2c). Successive laser heatings gradually promoted the transition (Figure 2d), and the initial C-RES eventually disappeared after about 10 mins heating at 1700 ± 200 K (Figure 2e). The transition phase was found to be identified as B-RES, the same phase reported in ref 7. The pressure slightly changed from 10.1 to 9.2 GPa as the transition proceeded; nevertheless, the transition pressure was in good agreement with the 11 GPa reported in the previous study.[7] After that, the pressure was completely released. The B-RES phase was recovered at ambient pressure (Figure 2f). C-RES did not transform during room-temperature compression to 31 GPa in a quasi-hydrostatic pressure medium (Figure 3). This suggests that the C- to B-RES transition may take place only at high temperatures or that it does not occur at room temperature because of a large kinetic barrier.

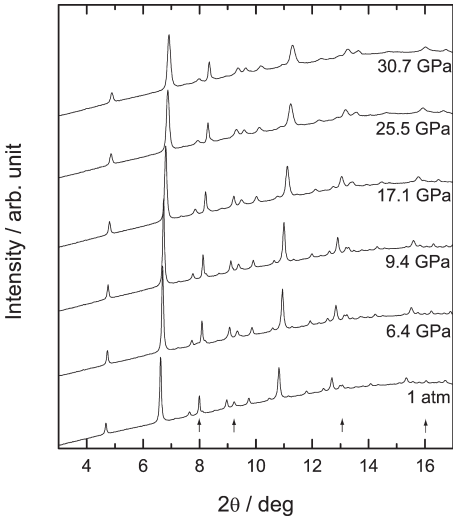

Figure 3. Variation in X-ray diffraction profiles from Sc_2O_3 samples with pressure under quasi-hydrostatic compression at room temperature. Monochromatic X-ray radiation of 38 keV was used. Arrows indicate the positions of diffraction from gold powder.

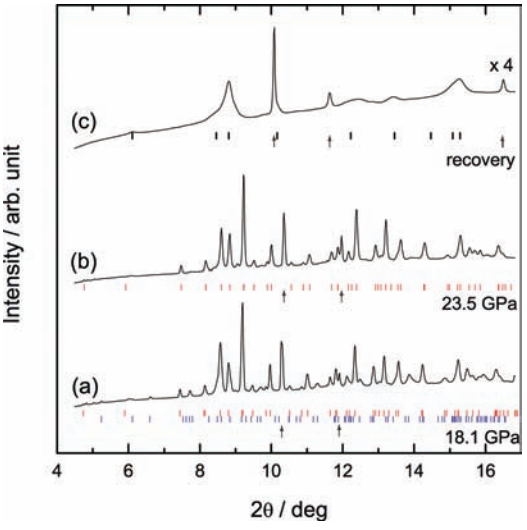

Figure 4. X-ray diffraction profiles from Sc_2O_3 samples (a) at 19.1 GPa after heating at 2000 ± 400 K, (b) at 23.5 GPa after heating at 2100 ± 350 K, and (c) after recovery at ambient pressure. Monochromatic X-ray radiation of 30 keV was used. Vertical bars represent the calculated positions of the diffraction peaks of the B-RES (lower bars) and Gd_2S_3 (upper bars) structures. Arrows indicate the positions of diffraction from gold powder. Bold vertical bars represent the calculated positions of the diffraction peaks of the corundum structure.

The second change appeared at 19.1 GPa at 2000 ± 400 K. Besides the appearance of a new phase, an untransformed B-RES phase showed up in the diffraction pattern (Figure 4a). During reheating at 23.5 GPa, the remnant B-RES phase was completely converted into the new phase (Figure 4b). We searched for the possible structure adoptable by this phase by referring to the known sesquioxide structures. We found that a Gd_2S_3 structure, which was recently found in In_2O_3 under high pressure,[21] appears to account for the new diffraction peaks. Because of the preferred orientation developed in the nonhydrostatic pressurized sample and spotty diffraction rings caused by grain growth during heating, Rietveld analysis for the collected diffraction patterns could not be directly

(27) Jamieson, J. C.; Fritz, J. N.; Manghnani, M. H. In *High-Pressure Research in Geophysics*; Center for Academic Publication Japan: Tokyo, 1982; pp 27−48.
(28) Morishima, H.; Yusa, H. *J. Appl. Phys.* **1998**, *83*, 1998.
(29) Hohenberg, P.; Kohn, W. *Phys. Rev.* **1964**, *136*, B864.
(30) Ceperley, D. M.; Alder, B. J. *Phys. Rev. Lett.* **1980**, *45*, 566.
(31) Perdew, J. P.; Zunger, A. *Phys. Rev B* **1981**, *23*, 5048.
(32) Perdew, J. P.; Burke, K.; Ernzerhof, M. *Phys. Rev. Lett.* **1996**, *77*, 3865.
(33) PWscf. http://www.pwscf.org (accessed Mar 2009).
(34) Vanderbilt, D. *Phys. Rev. B* **1990**, *41*, 7892.
(35) Monkhorst, H. J.; Pack, J. D. *Phys. Rev. B* **1976**, *13*, 5188.

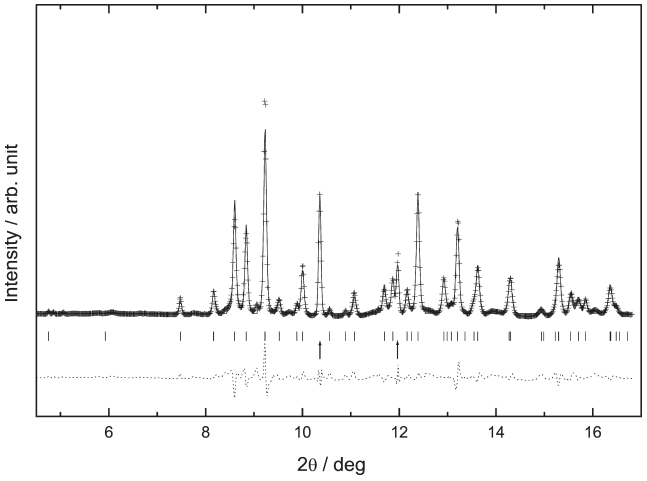

Figure 5. Powder X-ray diffraction patterns obtained with the LeBail method (GSAS) for a Gd_2S_3 structure in Sc_2O_3 at 23.5 GPa. Background was subtracted. The difference (dotted line) between the observed (crosses) and fitted patterns (thin line) is also shown on the same scale. Vertical bars represent the calculated positions of the diffraction peaks of the Gd_2S_3 structure. Arrows indicate the positions of diffractions from gold powder.

used to determine the atomic coordinates. Instead, the cell parameters were optimized by using the LeBail method in the GSAS package,[36] and the resulting lattice parameters were a = 5.4796(2) Å, b = 2.9796(3) Å, and c = 11.5479 (2) Å (R_{wp} = 0.038) at 23.5 GPa. Sufficiently small R_{wp} values and fitting errors indicate the validity of assignment to the Gd_2S_3 structure from the diffraction peaks (Figure 5). No other additional phase likely existed, because the X-ray profile at 19.1 GPa could be completely accounted for by the mixture of the B-RES and Gd_2S_3 phases (Figure 4a). In particular, no diffraction peaks corresponding to A-RES were found in any measured diffraction patterns. The calculated volume difference, $\Delta V_0 = (V_{\text{B-RES}} - V_{Gd_2S_3})/V_{\text{B-RES}}$, of 6.2% at 19.1 GPa is significantly larger than the typical volume difference between B- and A-RES, $\Delta V_0 = (V_{\text{B-RES}} - V_{\text{A-RES}})/V_{\text{B-RES}}$, which is ca. 1−2% in Sm_2O_3[37] and Eu_2O_3.[38] The appearance of the Gd_2S_3 phase with a large volume reduction might eclipse the A-RES phase in Sc_2O_3.

By repeating experiments, we confirmed that the Gd_2S_3 structure remained even at 65 GPa. Figure 6 plots all of the normalized volume data ($V/V_{0\text{C-RES}}$). After decompression, the diffraction peaks of the Gd_2S_3 phase became broad (Figure 4c). The peaks could be indexed by the corundum phase. Similar results were observed during decompression of the Gd_2S_3 phase in In_2O_3.[21] The volume change relative to the C-RES phase was ca. 3%, which is much smaller than the 6.2% volume difference between the C- and B-RES phases. It is interesting that the corundum phase, which has not previously been found in Sc_2O_3, can be synthesized only as a recovered product from the Gd_2S_3 phase.

The bulk moduli (B_0) of B-RES and the Gd_2S_3 phase were calculated to be 216 ± 8 GPa and 222 ± 14 GPa, respectively, by fitting the $P-V$ data to the third-order Birch−Murnaghan equation of state (B-M EOS) with a

(36) Larson, A. C.; Dreele, R. B. V. *Los Alamos National Laboratory Report LAUR*; Los Alamos National Laboratory: Los Alamos, NM, 2004; pp 86−748.

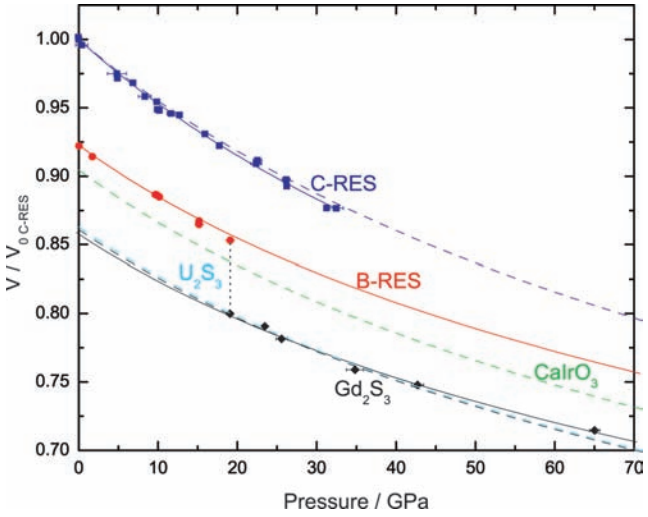

Figure 6. Compression curves and relative compression volume data (V/V_0) of C-RES (squares), B-RES (circles), and Gd_2S_3 (diamonds) phases. Solid lines are the results obtained by fitting the data to the Birch−Murnaghan equation of state. Broken lines are the results of DFT-LDA computations of C-RES, B-RES, $CaIrO_3$, U_2S_3, and Gd_2S_3 phases. A vertical dotted line shows the transition pressure to the Gd_2S_3 phase.

Table 1. Equation-of-State (EOS) Parameters (Zero-Pressure Bulk Modulus, B_0; Its Pressure Derivative, B_0'; and Cell Volume Per Formula Unit, V_0)

phase	V_0 (Å^3)	B_0 (GPa)	B_0'	method
C-RES	59.64			XRD[7]
	59.73(1)	189(7)	4.0(6)	XRD[a]
	57.24	199.0	3.85	DFT-LDA[a]
B-RES	55.02(8)			XRD[7]
	55.11(8)	216(8)	5[b]	XRD[a]
Gd_2S_3	51.16(31)	222(14)	5[b]	XRD[a]
	49.29	219.6	4.18	DFT-LDA[a]
U_2S_3	49.40	216.3	4.3	DFT-LDA[a]
$CaIrO_3$	51.78	211.2	4.19	DFT-LDA[a]

[a] Present work. [b] Fixed value is used.

fixed value of B_0'. The V_0 of the Gd_2S_3 phase can be obtained by extrapolation of the B-M EOS (Table 1). The total volume contraction $\Delta V_0 = (V_{\text{C-RES}} - V_{Gd_2S_3})/V_{\text{C-RES}}$ in Sc_2O_3 is 13.0%, which is in excellent agreement with the ΔV_0 of 13.3% in In_2O_3.[21]

Computational Results and Crystal Structures. Static enthalpy differences relative to C-RES for A-RES, corundum, Rh_2O_3(II), $CaIrO_3$, Gd_2S_3, and U_2S_3 were obtained for pressures up to 100 GPa within DFT combining LDA and GGA (Figure 7a,b). Both computations indicate a similar relationship between pressure and enthalpy for each phase, except for a small positive pressure shift in GGA, as is usually seen.[15,19] The first phase crossing the C-RES's enthalpy line is Gd_2S_3 with transition pressures at 11 GPa (LDA) and 18 GPa (GGA). No further crossovers exist on the Gd_2S_3's enthalpy line above these pressures. Although the calculations of B-RES were also performed, this structure never stabilized during structure relaxations at any pressures in Sc_2O_3. Experiments suggest that a possible reason for this is that the calculations are all static. As mentioned in the Experimental Results section, a high temperature is needed to advance the phase transformation from the C- to B-RES phase because the C-RES phase never crystallized into the B-RES phase under the compression

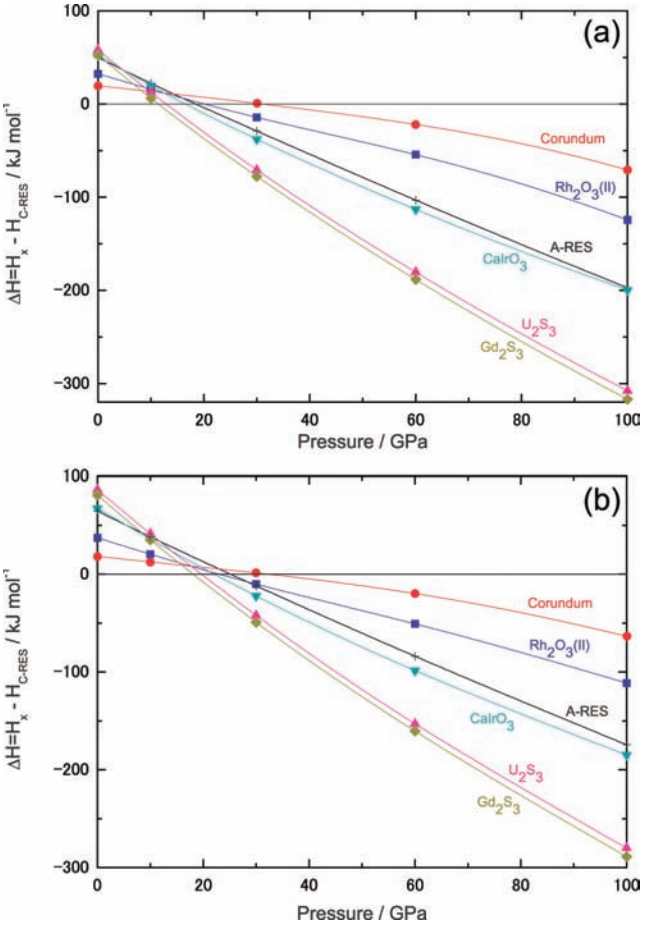

Figure 7. Enthalpy differences relative to C-RES for corundum (circles), Rh_2O_3(II) (squares), A-RES (crosses), $CaIrO_3$ (inverted triangles), U_2S_3 (triangles), and Gd_2S_3 (diamonds) in Sc_2O_3 by (a) DFT-LDA and (b) DFT-GGA computations under static conditions.

at room temperature. This suggests the stability range of the B-RES phase to be limited in the high-temperature region. Irrespective of the absence of the B-RES structure, the calculated static transition pressures of C-RES−Gd_2S_3 (11−18 GPa) are in harmony with experimental results (ca. 19 GPa).

Although the results of shock-compression experiments at 40.9 GPa[9] implied the existence of the A-RES phase, we did not find any evidence of stabilizing this phase in the entire pressure range of the DAC experiments. Being supportive of this, the present DFT calculations indicate that the enthalpy of A-RES is much higher than that of the Gd_2S_3 phase above the C-RES−Gd_2S_3 transition pressure. Note also that the recovered sample in ref 8 was not B-RES. If A-RES had formed under pressure, the recovered phase would have to be B-RES because the back transition from A- to B-RES is displacive, as reported in the case of some rare earth sesquioxides such as Sm_2O_3,[37] Eu_2O_3,[38] and Yb_2O_3.[39] Moreover, the estimated density change (11.5%) between C-RES and A-RES at ambient pressure in ref 8 is within acceptable error of the extrapolated density change (13.0%) between the C-RES and Gd_2S_3 phases in the present study. These considerations suggest that the high-pressure phase observed in the shock compression experiments would have likely been the Gd_2S_3 phase, not the A-RES phase.

(37) Guo, Q.; Zhao, Y.; Jiang, C.; Mao, W.; Wang, Z. *Solid State Commun.* **2008**, *145*, 250.
(38) Chen, G.; Peterson, J.; Brister, K. *J. Solid State Chem.* **1994**, *111*, 437.
(39) Fujimura, A.; Kikegawa, T.; Iwasaki, H. Unpublished results mentioned in ref 8.

Table 2. Lattice Parameters and Atomic Coordinates of Gd_2S_3 (*Pnma*; $Z = 4$) and U_2S_3 (*Pnma*; $Z = 4$) Phases at 30 GPa Determined by DFT-LDA Computations

phase	site	*x*	*y*	*z*
Gd_2S_3	Sc1	0.7643	0.25	0.5457
	Sc2	0.1516	0.25	0.2029
	O1	0.5140	0.25	0.1089
	O2	0.6440	0.25	0.7196
	O3	0.8681	0.25	0.9348
	lattice parameters	$a = 5.3565$ Å	$b = 2.9282$ Å	$c = 11.2681$ Å
U_2S_3	Sc1	−0.0075	0.25	0.3127
	Sc2	0.3084	0.25	0.5049
	O1	0.0470	0.25	0.8731
	O2	0.3816	0.25	0.9439
	O3	0.2298	0.25	0.1999
	lattice parameters	$a = 7.8831$ Å	$b = 2.9087$ Å	$c = 7.7173$ Å

Enthalpy of the Gd_2S_3 phase exhibits a pressure dependence similar to that of the U_2S_3 phase in the entirety of the pressure ranges within a difference less than 10 kJ mol^{-1}. As seen in their EOS parameters (Table 1), their compression curves (Figure 6) also show a similar trend, except for a slightly larger volume of the U_2S_3 phase. This similarity might be attributed to their structures with the same oxygen-coordination numbers, seven and eight. By looking carefully at the crystal structures in Figure 8, which are depicted using the atomic coordinates (Table 2) determined by the DFT-LDA computations, we can find distinct differences in their polyhedral connectivities. In the Gd_2S_3 structure, the ScO_8 bicapped trigonal prisms share the triangular faces of a pyramid along the *a* direction and also share the trigonal basal plane of the prism along the *b* direction. Another kind of oxygen-coordinated polyhedron, the ScO_7 monocapped trigonal prism, shares two pairs of edges with neighboring polyhedra in the *ab* plane. As a whole, the two-dimensionally connected ScO_8 and ScO_7 polyhedra form zigzag layers parallel to the *ab* plane. On the other hand, in the U_2S_3 structure, a pair of ScO_8 polyhedra, which share an edge of pyramids, form columnar structures sharing the faces of trigonal prisms along the *b* direction. Also, a pair of ScO_7 capped trigonal prisms make a columnar structure along the *b* direction by sharing their edges. Therefore, the U_2S_3 structure can be recognized as a complex columnar structure (Figure 8b), which is clearly different from the layered Gd_2S_3 structure (Figure 8a). Although both Gd_2S_3 and U_2S_3 structures possess monocapped and bicapped trigonal prisms as oxygen-coordinated polyhedra, we notice a difference in Sc−O distances in these polyhedra. Contrary to the small variation in Sc−O distances within 5% in the bicapped trigonal prism of the Gd_2S_3 structure, the variations in those of the U_2S_3 structure are significantly large (ca. 13%) due to a peculiar long distance of Sc2 to O3 (2.434 Å at 30 GPa). Thus, the coordination number of the bicapped trigonal prism in the U_2S_3 structure might not be 8 but rather (7 + 1). On the other hand, in their monocapped trigonal prism, the variations in Sc−O distances are found to be less than 6%.

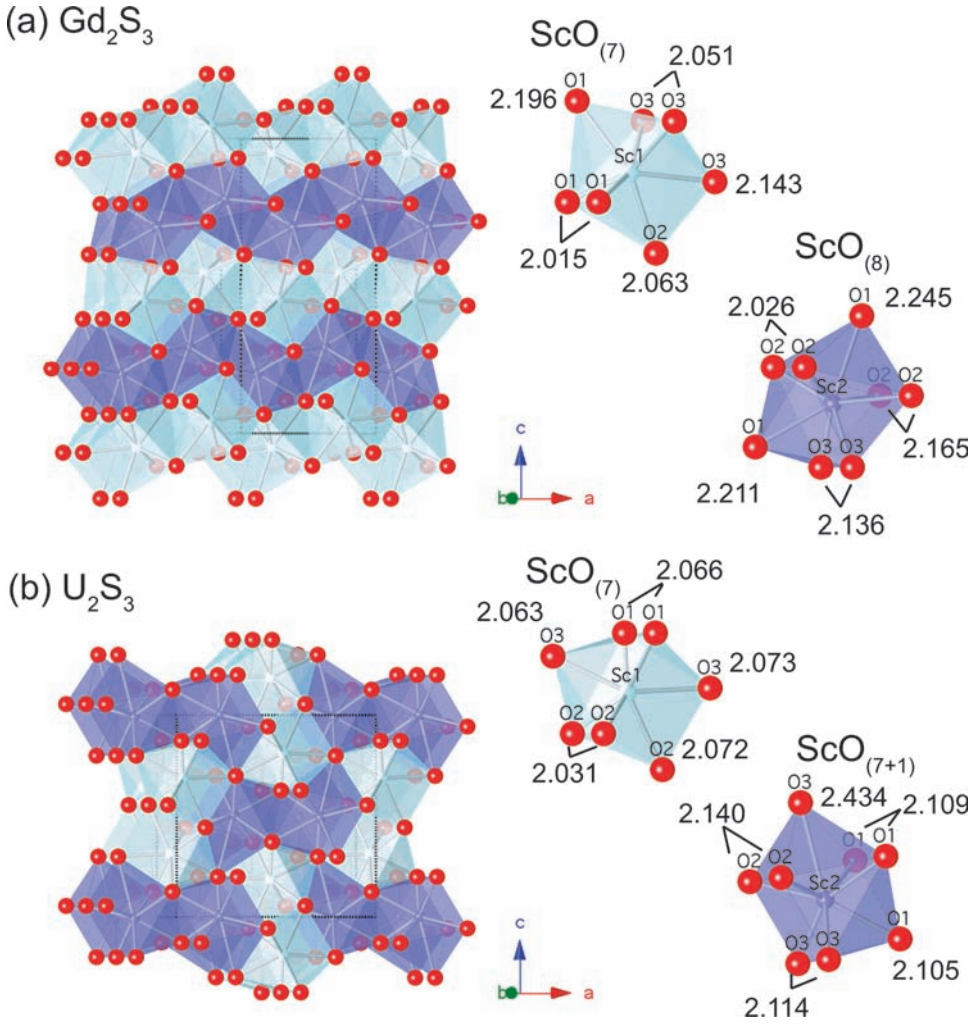

Figure 8. Clinographic view of crystal structures of (a) Gd_2S_3 and (b) U_2S_3 in Sc_2O_3 at 30 GPa. Large spheres are oxygen. Small spheres at the center of polyhedra are scandium. Unit cells are surrounded by dotted lines. Each type of polyhedra is depicted separately with Sc−O distances. The deeply colored polyhedra represent bicapped trigonal prisms with eight oxygen coordinations. Sc−O bond lengths are indicated by angstrom units.

Recent DFT calculations predicting the U_2S_3 phase as a post-$CaIrO_3$ phase of Al_2O_3 at 370 GPa suggested that the U_2S_3 phase was crystallographically similar to the $CaIrO_3$ phase; the structural change from the $CaIrO_3$ phase (*Cmcm*) to the U_2S_3 phase (*Pmcn*: third setting for comparison) can be simply explained by an elongation along the *a* and *c* directions and a compression along the *b* direction of the $CaIrO_3$ phase.[20] This suggests that, once the $CaIrO_3$ phase forms prior to the transition that increases the coordination number, it might easily transform into U_2S_3. In the case of Sc_2O_3, however, the $CaIrO_3$ phase did not appear. This might be one of the reasons why Sc_2O_3 prefers the Gd_2S_3 structure to the U_2S_3 structure as the higher oxygen-coordinated phase.

Comparative Crystallography in Rare Earth Sesquioxides and with Group 13 Sesquioxides. The phase sequence in Ln_2O_3 has been discussed on the basis of cationic radii[40] (Figure 9a) since Goldschmidt and his co-workers established the systematics from C- to B- and A-RES at elevated temperatures.[3] At the time, the C-to-B-RES transitions were confirmed from Nd^{3+} (0.983 Å) to Dy^{3+} (0.912 Å) sesquioxides at ambient pressure. Forty years later, an attempt to control the ionic size by using pressure opened a way to investigating further

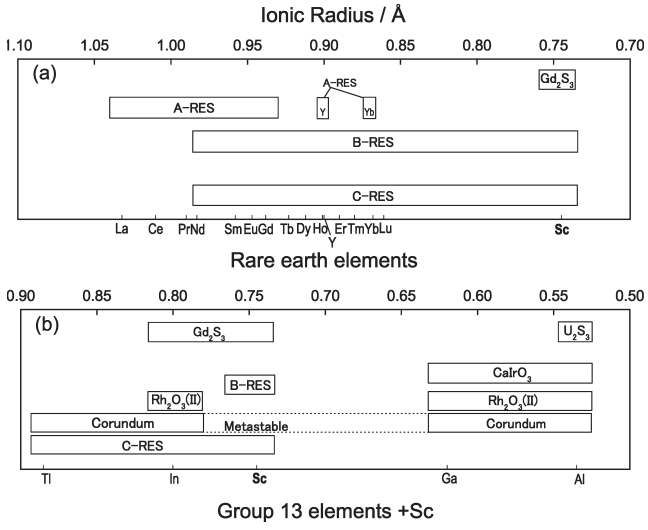

Figure 9. Variations of crystal structures in rare earth sesquioxides (a) and group 13 sesquioxides (b) summarized in terms of cationic radius.

(40) Shannon, R. D. *Acta Crystallogr., Sect. A* **1976**, *32*, 751. We quoted the trivalent cationic radii with six coordination number from this article.

systematics.[4−6] Then, the B-RES phases from Ho^{3+} (0.901 Å) to Lu^{3+} (0.861 Å) sesquioxides were successfully recovered by the high-pressure experiments up to 5 GPa at high temperatures.[6] On the other hand, it was reported that only larger cations, La^{3+} (1.032 Å) through Nd^{3+} (0.983 Å), crystallized into A-RES phases at ambient pressure. Unlike the reconstructive C-to-B-RES transition, the B-to-A-RES transition is displacive. A-RES reverts to B-RES during decompression, so that we could not obtain direct information about the transition any more after releasing the pressure in the high-pressure experiments. Only a trace of the transition was detected as a disordered feature of the B-RES phase.[8] Recent progress in high-pressure in situ observation techniques has thrown light on the unquenchable A-RES phase. In compression experiments conducted at room temperature, A-RES phases with intermediate cations Sm^{3+} (0.958 Å),[37,41−43] Eu^{3+} (0.947 Å),[38] Gd^{3+} (0.938 Å),[42,44] and Yb^{3+} (0.900 Å)[39] were confirmed by in situ X-ray diffraction or Raman scattering at 2.5−4.7, 4.7, 5.2−10.3, and 15 GPa, respectively. These results suggest that higher pressures would be needed to crystallize the A-RES phase in Ln_2O_3 with a smaller cationic radius.

It is a good question whether the systematics are applicable to the other sesquioxides or not. One of the rare earth sesquioxides, Y_2O_3 (Y^{3+}; 0.900 Å), which has a cationic radius similar to that of lanthanoid Ho^{3+} (0.901 Å), undergoes C-to-B-RES and B-to-A-RES transitions at 12 and 19 GPa, respectively,[45] and reflects the systematics of Ln_2O_3. Of the group 13 sesquioxides, no RES phases have been found in Al^{3+} (0.535 Å) and Ga^{3+} (0.620 Å),[11−17] as clearly shown in Figure 9b. The C-RES phase appears as an ambient phase in In_2O_3, where the cationic radius of In^{3+} (0.800 Å) is rather smaller than that of Lu^{3+} (0.861 Å). By extrapolating the pressure versus cationic radius line of their results, Hoekstra predicted a C-to-B-RES transition in In_2O_3 at a pressure of more than 7.5 GPa.[6] However, our previous study revealed not the B-RES phase but, rather, the corundum and the Rh_2O_3(II) phases at about 7 GPa.[14] At pressures above 40 GPa, we discovered a new dense Gd_2S_3 structure,[21] which is denser than not only the B- and A-RES phases but also the $CaIrO_3$ phase. Although the ionic radius of Sc^{3+} (0.745 Å) is much smaller than that of In^{3+} (0.800 Å), the C-to-B-RES transition takes place at 10.1 GPa in Sc_2O_3. If we apply the Hoekstra's pressure verses cationic radius line to the ionic radius of Sc^{3+}, the expected transition pressure would be 11 GPa, which is in remarkable agreement with our experimental value. However, a further transition from the B- to A-RES phase expected in analogy to Ln_2O_3 was not observed in Sc_2O_3; instead, the B-RES phase directly transformed into an unquenchable Gd_2S_3 phase at 19 GPa. These conflicting results suggest that the systematics of the phase sequence of Ln_2O_3 are not simply applicable to all sesquioxides only in connection with their cationic radii. The cations smaller than 0.85 Å seem highly unlikely to stabilize the A-RES sesquioxides structure.

Irrespective of electronic configuration, the Gd_2S_3 structure appears in both indium and scandium sesquioxides. Under the lower pressure, the structure would be dominated by the individual character of cations, as indicated in the example that In^{3+} prefers corundum and Rh_2O_3(II) structures to the B-RES structure. The character would likely be lost with increasing pressure, so that both In^{3+} and Sc^{3+} crystallize the Gd_2S_3 structure. The large density jumps and the oxygen coordinated number increases accompanied with the transition to Gd_2S_3 would make this structure quite reasonable under high pressure. Also, such structural changes are clearly responsible to the density functional static enthalpy relationships. Although the U_2S_3 structure was predicted for Al_2O_3,[20] we never found it in Sc_2O_3 or In_2O_3. This fact implies that sesquioxides generally prefer the Gd_2S_3 structure to the U_2S_3 structure. It is highly possible that the new transition systematics to the Gd_2S_3 structure would be universal in most sesquioxides beyond the A-RES phase. Further and extensive investigations into the post-A-RES structure under high $P-T$ conditions will develop these new systematics.

Summary

The present study proved that B-RES-type scandium sesquioxide undergoes a high-pressure phase transition to the Gd_2S_3 structure, not to A-RES. The considerable increase in density eclipses the appearance of the $CaIrO_3$ phase. Both experimental and computational results demonstrated that the U_2S_3 structure does not stabilize in Sc_2O_3, unlike results from a recent report on Al_2O_3. This discovery of a dense Gd_2S_3 structure in Sc_2O_3 suggests new systematics for the high-pressure phase sequence in sesquioxides.

Acknowledgment. The synchrotron radiation experiments were conducted at BL-10XU of SPring-8 with the approval of JASRI (Proposal Nos. 2008A1253, 2007B1147, and 2007B1192). H.Y. acknowledges support from NIMS Competitive Research Funds. T.T. acknowledges supports from a Grant-in-Aid for Scientific Research from JSPS (No. 19740331).

(41) Atou, T.; Kusaba, K.; Tsuchida, Y.; Utsumi, W.; Yagi, T.; Syono, Y. *Mater. Res. Bull.* **1989**, *24*, 1171.
(42) Atou, T.; Kusaba, K.; Syono, Y.; Kikegawa, T.; Iwasaki, H. In *High-Pressure Research Application to Earth and Planetary Sciences*; Terra Pub.: Tokyo, 1992; pp 469−475.
(43) Hongo, T.; Kondo, K.; Nakamura, K. G.; Atou, T. *J. Mater. Sci.* **2007**, *42*, 2582.
(44) Chen, H.; He, C.; Gao, C.; Ma, Y.; Zhang, J.; Wang, X.; Gao, S.; Li, D.; Kan, S.; Zou, G. *J. Phys.: Condens. Matter* **2007**, *19*, 425229.
(45) Husson, E.; Proust, C.; Gillet, P.; Itie, J. P. *Mater. Res. Bull.* **1999**, *34*, 2085.